Multi-channel Deep Transfer Learning for Nuclei Segmentation in Glioblastoma Cell Tissue Images

Thomas Wollmann[1], Julia Ivanova[1], Manuel Gunkel[2], Inn Chung[3],
Holger Erfle[2], Karsten Rippe[3], Karl Rohr[1]

[1] University of Heidelberg, BioQuant, IPMB, and DKFZ Heidelberg, Dept.
Bioinformatics and Functional Genomics, Biomedical Computer Vision Group,
[2] High-Content Analysis of the Cell (HiCell) and Advanced Biological Screening
Facility, BioQuant, University of Heidelberg, Germany
[3] Division of Chromatin Networks, DKFZ and BioQuant, Heidelberg, Germany
`thomas.wollmann@bioquant.uni-heidelberg.de`

Abstract. Segmentation and quantification of cell nuclei is an important task in tissue microscopy image analysis. We introduce a deep learning method leveraging atrous spatial pyramid pooling for cell segmentation. We also present two different approaches for transfer learning using datasets with a different number of channels. A quantitative comparison with previous methods was performed on challenging glioblastoma cell tissue images. We found that our transfer learning method improves the segmentation result.

1 Introduction

Segmentation of cell nuclei is a frequent and important task in quantitative microscopy image analysis and for extracting phenotypes. In this work, we consider the segmentation of nuclei from 3D tissue microscopy images of glioblastoma cells. This data is very challenging due to strong intensity variation, cell clustering, poor edge information, missing object borders, strong shape variation, and low signal-to-noise ratio (Fig. 1).

In previous work, several methods for cell segmentation were introduced (e.g., [1, 2]). Recently, deep learning methods achieved very good results [2]. When only a small dataset is available for training, it is common in video image analysis of natural scenes to pretrain a deep neural network on a large dataset like ImageNet and fine-tune the network on the considered dataset [3]. However, images of natural scenes are usually color images represented by three channels, but microscopy images generally have a varying number of channels (and often more than three channels). For a convolutional neural network, in the first layer a filter is used for each channel to extract corresponding feature maps. Hence, the number of channels is fixed in the network according to the considered data, and the pretrained network cannot directly be transferred to data with a different number of channels.

In this work, we introduce a novel deep neural network based on atrous spatial pyramid pooling (ASPP) for cell segmentation. We also present two transfer learning approaches which use only one channel for training and perform fine-tuning on more channels. In our application, we trained the neural network on a one-channel dataset and transfer it to a dataset with four channels. We applied our method to segment cell nuclei in challenging glioblastoma cell tissue images and performed a quantitative comparison with previous methods.

2 Methods

Our proposed deep learning method combines a U-Net [2] with batch normalization [4], residual connections [5], and atrous spatial pyramid pooling (ASPP) [6]. ASPP has the advantage that large context information can be captured at multiple image scales. We modified ASPP by using dilations of 1, 2, and 4 as well as global average pooling (pooling kernel equal to feature maps) to capture information from the whole image. After the ASPP block we employ Gaussian dropout (p=0.5). For our deep learning model we investigated PReLU [7] activation functions. Using a U-Net in conjunction with a PReLU activation function, we observed that the first layers mostly favour negative activations. However, PReLU increases the computation time. Therefore, we used PReLU only in the first layer to make use of negatively activated features, while saving computation time.

Our network was trained using cross-validation and early stopping with the Adam optimizer and a learning rate of $l_{init} = 0.001$ as well as $\beta_1 = 0.9$ and $\beta_2 = 0.999$. The dataset was always split into 50 % training, 25 % validation, and 25 % testing data. We augmented the dataset using random flipping, rotation, cropping (200×200 pixels), color shift, and elastic deformations.

(a) Original image   (b) Manual annotation
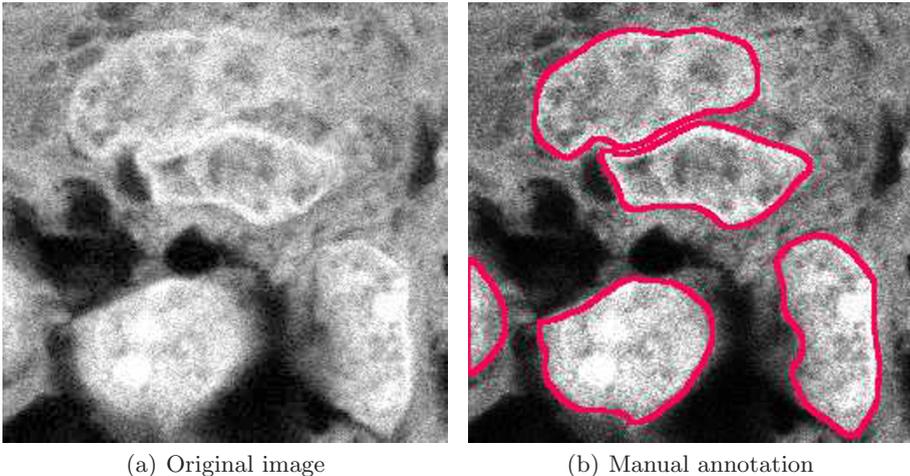
Fig. 1. DAPI channel of original tissue image of glioblastoma cells and ground truth annotation.

For transfer learning we employed two approaches. In the first approach, we use the network trained on one channel (Fig. 2(a)) for all channels by altering the first layer of the network and using the same trained convolutional filters for all channels (Fig. 2(b)). This is motivated by the assumption that the trained filters are generic for different types of images and can therefore be applied to other channels with different stainings. In the second approach, we use the trained convolutional filters for the corresponding channel in the new dataset and initialize the filters for the other channels by MSRA initialisation [7] (Fig. 2(c)). With this approach we keep the pretrained filters for one channel and train all other filters from scratch.

2.1   Performance measures

We used four performance measures for quantitative evaluation: Object IOU, IOU, Dice, and Warping Error. The object-based intersection over union (Object IOU) measure quantifies the agreement between the segmentation result and the ground truth for each object. We matched a ground truth object to a segmented object, if the normalized overlap is more than 50 %. In addition to this object-based IOU, we also determined a pixel-based IOU. The Dice coefficient is defined as the ratio of true positive pixels and the sum of pixels in ground truth and segmentation. The Warping Error [8] is the minimum mean square error between pixels of the segmentation and pixels of the topology-preserving warped ground truth. We calculated all performance measures for each image and averaged over the whole dataset.

3   Experimental results

We applied our method to tissue microscopy images of glioblastoma cells. Segmentation of cell nuclei is important for subsequent analysis of telomeres and for patient stratification [9]. The dataset consists of five 3D images and was acquired
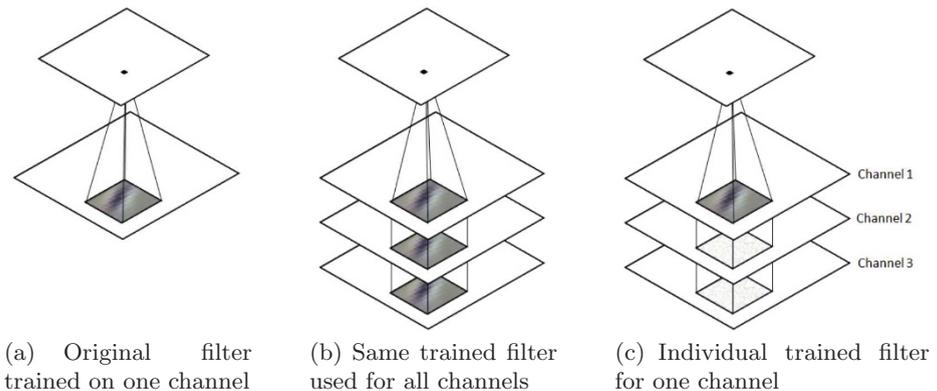

(a)   Original   filter trained on one channel

(b) Same trained filter used for all channels

(c) Individual trained filter for one channel

Fig. 2. Different approaches for transfer learning.

Table 1. Performance of different segmentation methods. Bold and underline highlights the best result, and bold indicates the second best result.

Method	Object IOU	IOU	Dice	Warp Error [10^{-4}]
Clustering & Thresholding	0.5782	**<u>0.6520</u>**	**<u>0.7884</u>**	0.093
Fast-Marching Level Set	0.5065	0.5682	0.7194	0.149
U-Net	0.6666	0.5774	0.7168	**<u>0.011</u>**
Proposed NN	0.7814	0.6154	0.7581	0.040
Proposed NN (transfer, same filter)	**0.7913**	0.5221	0.6709	0.045
Proposed NN (transfer, indiv. filters)	**<u>0.7981</u>**	**0.6426**	**0.7775**	**0.030**

by a Leica TCS SP5 point scanning confocal microscope with a 63x objective lens and a voxel size of $100 \times 100 \times 250$ nm. Four color channels were imaged sequentially: PML antibody stain (Alexa 647), FISH CY3 telomere probe, FAM labeled CENP-B PNA probe, and DAPI nuclei stain. 45 axial sections were acquired for each 3D stack. The deep learning models with transfer learning were trained on a second dataset with glioblastoma cells containing 50 images stained with DAPI nuclei stain, before training on the considered first dataset. However, the second dataset has only one channel and consists of maximum intensity projection (MIP) images. Therefore, standard transfer learning is not applicable and we need other approaches such as the two transfer learning strategies described in Section 2 above.

For a quantitative comparison, we also applied thresholding in combination with mean shift clustering. The 3D images were preprocessed using 3D Gaussian filtering ($\sigma = 2$ pixels). We used an empirically determined threshold of 160. In addition, we used an approach based on Gaussian filtering, mean shift clustering, and 3D fast-marching level sets [10]. The segmentation results were post-processed using hole filling.

All segmentation methods were evaluated on the 3D images from the first dataset, which were not used for training. We compared the segmentation results for five 3D images each containing 65 sections (in total 325 2D images per channel were used). Ground truth segmentations for all images were determined by manual annotation. Table 1 shows the results for all methods for the different evaluation metrics. It turns out that the proposed neural network combined with transferring individual filters performs best for object-based IOU and second best for IOU, Dice and Warping Error. Segmentation results for an example image are provided in Fig. 3. It can be seen that the proposed network performs best. In addition, transferring individual filters improves cell separation. The high object-based IOU and low Warping Error indicates that the proposed model is more suited to correctly merge and split objects.

4   Conclusion

We presented a deep neural network based on ASPP for cell segmentation combined with two approaches for transfer learning to transfer trained networks from

one-channel data to multi-channel data. Based on a quantiative comparison using glioblastoma cell tissue images we showed that transfer learning improves the performance. Our novel deep neural network in conjunction with transfer learning and individual filters performed best for Object IOU and second best for Dice and Warping Error.

(a) Original image   (b) Ground truth   (c) Cluster. & Thresholding

(d) Fast-Marching Level Set   (e) U-Net   (f) Proposed NN

(g) Proposed NN (transfer, same filter)   (h) Proposed NN (transfer, individual filters)
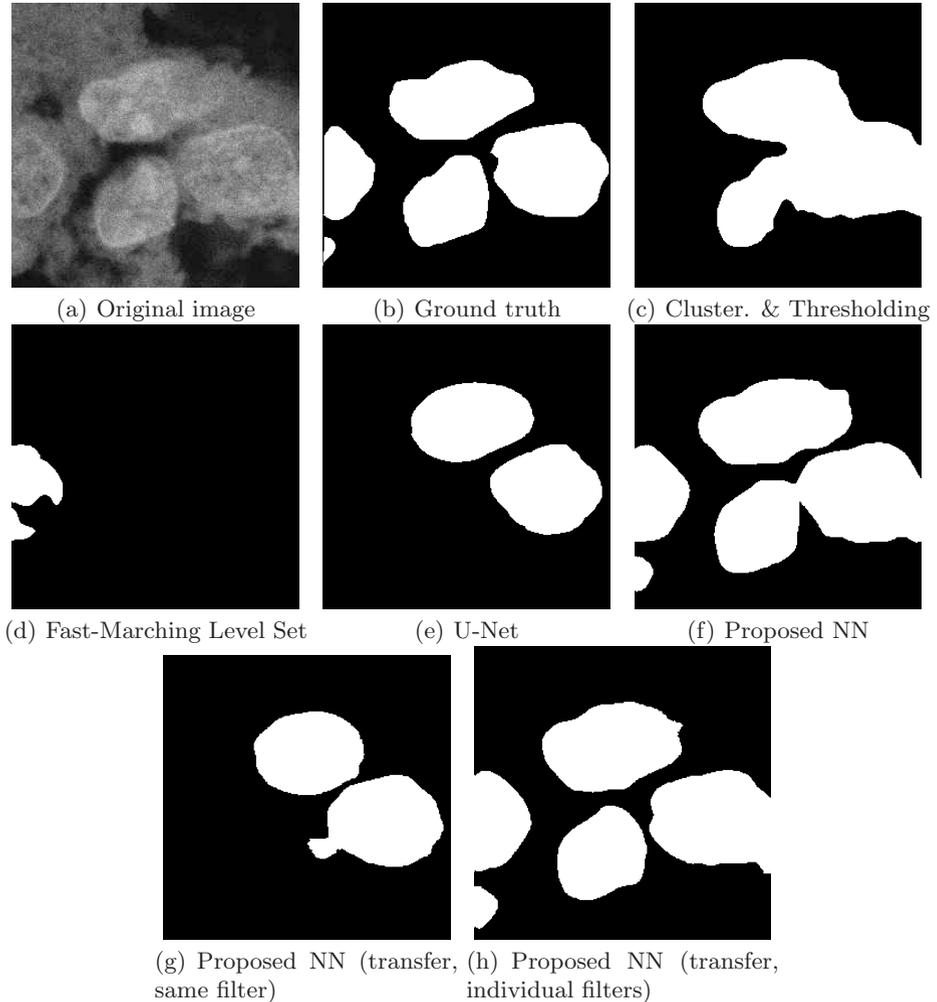
Fig. 3. Example tissue microscopy image of glioblastoma cells, ground truth, and segmentation results of different methods.

References

1. Dima AA, Elliott JT, Filliben JJ, et al. Comparison of segmentation algorithms for fluorescence microscopy images of cells. Cytometry Part A. 2011;79(7):545–559.
2. Ronneberger O, Fischer P, Brox T. U-Net: convolutional networks for biomedical image segmentation. Proc MICCAI. 2015; p. 234–241.
3. Huh M, Agrawal P, Efros AA. What makes ImageNet good for transfer learning?. arXiv:1608.08614; 2016.
4. Ioffe S, Szegedy C. Batch normalization: Accelerating deep network training by reducing internal covariate shift. Proc ICML. 2015; p. 448–456.
5. He K, Zhang X, Ren S, et al. Deep residual learning for image recognition. Proc CVPR. 2016; p. 770–778.
6. Chen LC, Papandreou G, Kokkinos I, et al.. Deeplab: Semantic image segmentation with deep convolutional nets, atrous convolution, and fully connected CRFs. arXiv:1606.00915; 2016.
7. He K, Zhang X, Ren S, et al. Delving deep into rectifiers: Surpassing human-level performance on imagenet classification. Proc ICCV. 2015; p. 1026–1034.
8. Jain V, Bollmann B, Richardson M, et al. Boundary learning by optimization with topological constraints. Proc CVPR. 2010; p. 2488–2495.
9. Osterwald S, Deeg KI, Chung I, et al. PML induces compaction, TRF2 depletion and DNA damage signaling at telomeres and promotes their alternative lengthening. J Cell Sci. 2015;128(10):1887–1900.
10. Sethian JA. Level Set Methods and Fast Marching Methods. vol. 3. Cambridge University Press; 1999.